

# Remote Sensing of Sea Ice in the Northern Sea Route

Studies and Applications

---

Ola M. Johannessen, Vitaly Yu. Alexandrov,  
Ivan Ye. Frolov, Stein Sandven, Lasse H. Pettersson,  
Leonid P. Bobylev, Kjell Kloster, Vladimir G. Smirnov,  
Yevgeny U. Mironov and Nikolay G. Babich

---

# Remote Sensing of Sea Ice in the Northern Sea Route

**Studies and Applications**

 Springer

Published in association with  
**Praxis Publishing**  
Chichester, UK

PRAXIS 

Professor Ola M. Johannessen  
Founding Director  
Nansen Environmental and Remote Sensing Center  
Mohn-Sverdrup Center for Global Ocean Studies  
and Operational Oceanography  
Geophysical Institute, University of Bergen,  
Bergen, Norway

Mr. Lasse H. Pettersson  
Mr. Kjell Kloster  
Nansen Environmental and Remote Sensing Center  
Bergen, Norway

Dr. Leonid P. Bobylev  
Nansen International Environmental and Remote  
Sensing Center  
St. Petersburg, Russia  
Nansen Environmental and Remote Sensing Center  
Bergen, Norway

Mr. Nikolay G. Babich  
Murmansk Shipping Company  
Murmansk, Russia

Professor Stein Sandven  
Nansen Environmental and Remote Sensing Center  
Bergen, Norway  
University Courses on Svalbard—UNIS,  
Longyearbyen, Norway

Dr. Vitaly Yu. Alexandrov  
Nansen International Environmental and Remote  
Sensing Center  
St. Petersburg, Russia

Professor Ivan Ye. Frolov  
Dr. Vladimir G. Smirnov  
Dr. Yevgeny U. Mironov  
Arctic and Antarctic Research Institute (AARI)  
St. Petersburg, Russia

---

SPRINGER-PRAXIS BOOKS IN GEOPHYSICAL SCIENCES

SUBJECT *ADVISORY EDITOR*: Dr Philippe Blondel, C.Geol., F.G.S., Ph.D., M.Sc., Senior Scientist,  
Department of Physics, University of Bath, Bath, UK

Published in association with the Nansen Centers in Bergen and St. Petersburg  
Nansen Center's Polar Series No. 4

---

ISBN 10: 3-540-24448-4 Springer-Verlag Berlin Heidelberg New York

Springer is part of Springer-Science + Business Media ([springer.com](http://springer.com))

Bibliographic information published by Die Deutsche Bibliothek

Die Deutsche Bibliothek lists this publication in the Deutsche Nationalbibliografie;  
detailed bibliographic data are available from the Internet at <http://dnb.ddb.de>

Library of Congress Control Number: 2006924127

Apart from any fair dealing for the purposes of research or private study, or criticism or review, as permitted under the Copyright, Designs and Patents Act 1988, this publication may only be reproduced, stored or transmitted, in any form or by any means, with the prior permission in writing of the publishers, or in the case of reprographic reproduction in accordance with the terms of licences issued by the Copyright Licensing Agency. Enquiries concerning reproduction outside those terms should be sent to the publishers.

© Praxis Publishing Ltd, Chichester, UK, 2007  
Printed in Germany

The use of general descriptive names, registered names, trademarks, etc. in this publication does not imply, even in the absence of a specific statement, that such names are exempt from the relevant protective laws and regulations and therefore free for general use.

Cover design: Jim Wilkie

Project management: Originator Publishing Services, Gt. Yarmouth, Norfolk, UK

Printed on acid-free paper

# Contents

<b>Preface</b> . . . . .	ix
<b>Acknowledgments</b> . . . . .	xiii
<b>List of figures</b> . . . . .	xv
<b>List of tables</b> . . . . .	xxiii
<b>List of abbreviations</b> . . . . .	xxvii
<b>List of authors</b> . . . . .	xxxi
<b>List of contributing authors</b> . . . . .	xxxiii
<b>Introduction</b> . . . . .	xxxvii
<b>1 History of the Northern Sea Route</b> . . . . .	1
1.1 First voyages . . . . .	1
1.2 Voyages in the 16th–17th centuries . . . . .	2
1.3 From the 18th to the early 20th century . . . . .	6
1.3.1 Expeditions and geographical discoveries . . . . .	6
1.3.2 Beginning of trade shipping . . . . .	13
1.4 The Soviet–Russian system for supporting navigation . . . . .	14
<b>2 Sea ice conditions in the Arctic and in the Northern Sea Route</b> . . . . .	25
2.1 Sea ice conditions in the Arctic Ocean . . . . .	25
2.1.1 Seasonal changes . . . . .	25
2.1.2 Ice drift and its spatial and temporal variability . . . . .	29
2.1.3 Ice cover distribution . . . . .	37

2.2	The Arctic Eurasian Shelf seas . . . . .	44
2.2.1	Ice formation and ice thickness growth . . . . .	46
2.2.2	Ice exchange of the Arctic seas with the Arctic Basin. . .	54
2.2.3	Landfast ice and polynyas of the Arctic seas . . . . .	58
2.2.4	Ice distribution during ice cover decay . . . . .	60
<b>3</b>	<b>Sea ice monitoring</b> . . . . .	<b>65</b>
3.1	History of ice monitoring in the Northern Sea Route . . . . .	65
3.1.1	Airborne ice reconnaissance (1924–1932) . . . . .	66
3.1.2	Visual observations of sea ice from aircraft (1933–1950) .	68
3.1.3	Development of aircraft and satellite remote sensing (1951–1984) . . . . .	73
3.1.4	The <i>Okean</i> radar satellite . . . . .	91
3.1.5	Creation and development of an automated ice information system for the Arctic (1975–1991) . . . . .	99
3.1.6	Satellite synthetic aperture radar . . . . .	101
3.1.7	Passive microwave radiometry . . . . .	109
3.2	Operational sea ice monitoring in the Northern Sea Route . . . .	116
3.2.1	Organization of monitoring. . . . .	116
3.2.2	Information support for users . . . . .	118
3.3	User requirements for sea ice information on the Northern Sea Route . . . . .	122
3.3.1	General survey of users . . . . .	122
3.3.2	Sea ice information for navigation support. . . . .	127
3.3.3	Role of satellite earth observation (EO) data . . . . .	133
3.4	Operational sea ice services in other Arctic countries . . . . .	137
3.4.1	Introduction. . . . .	137
3.4.2	The International Ice Patrol . . . . .	139
3.4.3	The U.S. National Ice Center . . . . .	139
3.4.4	The Canadian Ice Service . . . . .	140
3.4.5	The Danish Ice Service for Greenland waters . . . . .	143
3.4.6	The Icelandic Ice Service . . . . .	143
3.4.7	The Norwegian Ice Service for Arctic waters . . . . .	145
3.4.8	Other Arctic ice monitoring services . . . . .	145
<b>4</b>	<b>Satellite remote sensing of sea ice</b> . . . . .	<b>149</b>
4.1	Optical and infrared imaging . . . . .	149
4.1.1	Satellites and sensors . . . . .	149
4.1.2	Processing of optical satellite images. . . . .	151
4.1.3	Interpretation of sea ice types and features . . . . .	156
4.1.4	Retrieval of sea ice thickness from infrared images . . . .	164
4.2	Radar imaging . . . . .	171
4.2.1	Imaging radar systems . . . . .	173
4.2.2	Signal calibration, corrections and adjustment . . . . .	178
4.2.3	Radar backscatter from sea ice . . . . .	182

4.3	Interpretation of sea ice parameters in SAR images . . . . .	191
4.3.1	Ice development . . . . .	192
4.3.2	Forms of fast ice . . . . .	201
4.3.3	Forms of floating ice . . . . .	202
4.3.4	Ice edge . . . . .	202
4.3.5	Openings in the sea ice . . . . .	209
4.3.6	Ice surface deformations. . . . .	212
4.3.7	Icebergs . . . . .	216
4.4	Sea ice retrieval algorithms for SAR . . . . .	220
4.4.1	Sea ice classification . . . . .	221
4.4.2	Sea ice concentration . . . . .	233
4.4.3	Sea ice motion . . . . .	239
4.5	Ice chart composition at AARI . . . . .	243
4.5.1	Generation of ice charts from optical images . . . . .	244
4.5.2	Generation of ice charts from SAR images . . . . .	246
<b>5</b>	<b>Sea ice conditions observed from satellite remote-sensing data . . . . .</b>	<b>253</b>
5.1	Western part of the Northern Sea Route . . . . .	253
5.1.1	Ice edge position. . . . .	254
5.1.2	Ice massifs. . . . .	257
5.1.3	Fast ice distribution . . . . .	264
5.1.4	Flaw polynyas . . . . .	270
5.1.5	Fractures in the sea ice . . . . .	274
5.2	Eastern part of the Northern Sea Route . . . . .	280
5.2.1	Ice edge position. . . . .	281
5.2.2	Ice massifs. . . . .	283
5.2.3	Ice drift variability based on remote-sensing observations . . . . .	286
5.2.4	Fast ice distribution . . . . .	290
5.2.5	Flaw polynyas . . . . .	297
5.3	SAR studies of Sea Ice conditions . . . . .	300
5.3.1	Fast ice. . . . .	301
5.3.2	Coastal polynyas. . . . .	306
5.3.3	Ice drift in the Laptev Sea . . . . .	310
<b>6</b>	<b>Application of SAR for ice navigation in the Northern Sea Route. . . . .</b>	<b>323</b>
6.1	Use of SAR images during expeditions—pre- <i>Envisat</i> . . . . .	323
6.1.1	The first SAR ice routing experiment with <i>L'Astrolabe</i> in 1991. . . . .	325
6.1.2	Voyages in the period 1993/1994 . . . . .	332
6.1.3	The <i>Kandalaksha</i> voyage from Japan to Norway. . . . .	343
6.1.4	The Icewatch expedition in winter 1996. . . . .	346
6.1.5	First use of <i>Radarsat</i> on <i>Sovetsky Soyuz</i> during summer 1997. . . . .	347
6.1.6	The Ice Routes and ARCDEV expeditions in 1998 . . . . .	350

6.2	<i>Envisat</i> ASAR period from 2003 . . . . .	358
6.2.1	<i>Envisat</i> demonstration in summer 2003 . . . . .	358
6.2.2	Winter–spring 2004 . . . . .	359
6.2.3	<i>Envisat</i> demonstrations, winter–spring 2005 . . . . .	365
6.3	Use of SAR data onboard icebreakers . . . . .	368
6.3.1	Processing of SAR images and transmission to icebreakers . . . . .	368
6.3.2	Use of SAR data onboard icebreakers for route selection . . . . .	371
6.4	Use of optical images onboard icebreakers . . . . .	373
6.5	Ice routing and assessment of satellite images . . . . .	377
6.6	Future development of sea ice monitoring . . . . .	381
6.6.1	Prospective satellite systems . . . . .	381
6.6.2	Use of airborne and <i>in situ</i> systems . . . . .	386
6.6.3	Combined use of different remote-sensing data . . . . .	392
<b>7</b>	<b>Climatic variability of sea ice in the Arctic . . . . .</b>	<b>397</b>
7.1	Long-term variability of sea ice in the Eurasian Arctic . . . . .	398
7.1.1	Sea ice data . . . . .	398
7.1.2	Linear trends in sea ice extent . . . . .	399
7.1.3	Quasi-periodic variability of sea ice extent . . . . .	403
7.1.4	Causes of quasi-periodic fluctuations in ice extent . . . . .	407
7.2	Recent Arctic sea ice variability from satellite data . . . . .	409
7.2.1	Arctic sea ice concentration, area and extent, 1978–present . . . . .	409
7.2.2	Thick multi-year ice area . . . . .	412
7.3	21st century sea ice scenarios: statistical modeling . . . . .	418
7.4	21st century sea ice scenarios: numerical modeling . . . . .	420
7.4.1	Numerical model predictions . . . . .	420
7.4.2	Climate and its implications for the Northern Sea Route . . . . .	421
<b>8</b>	<b>Afterword . . . . .</b>	<b>423</b>
	<b>Glossary of sea ice terms . . . . .</b>	<b>427</b>
	<b>References . . . . .</b>	<b>435</b>
	<b>Index . . . . .</b>	<b>465</b>

# Preface

The Northern Sea Route (NSR) consists of the sailing routes in the Russian Arctic between the Barents Sea in the west and the Bering Strait in the east (Figure 1). It is the shortest sailing route linking northwestern Europe and northeastern Asia. The distance between Yokohama and Hamburg is almost half of that through the Suez Canal and 10–14 days in sailing time can be saved using the northern route. However, the presence of sea ice significantly hampers navigation. In winter the sailing routes are covered with ice, and even in summer some parts are ice-covered, especially in the Laptev and East Siberian Seas. Therefore, a fleet of conventional and nuclear Russian icebreakers supports safe and cost-effective ship transportation during the different seasons.

Hydrometeorological information, including sea ice data, is accordingly an essential and integral part of navigation safety. Therefore, the Northern Sea Route Administration, founded in 1932, established a service of hydrometeorological support for the region.

From the start of this service, polar aviation began ice reconnaissance to support all shipping transport in the Arctic. By 1935, all foreign aircraft—except *Dornier Wal* seaplanes which were used for ice reconnaissance until 1945—were replaced by aircraft manufactured in Russia. In the 1950s, visual airborne ice reconnaissance continued to be the main tool for sea ice monitoring and hydrometeorological services for Arctic navigation. Annually, 30–40 Russian aircraft carried out 500–700 ice reconnaissance flights. In 1964, the scientific and manufacturing association NPO Leninets began developing SLAR specifically for ice reconnaissance. In summer of 1966 AARI obtained the first TV images from *ESSA-2* and *Meteor-1*. In 1975 the first satellite of the Russian *Meteor-2* series was launched and used for sea ice monitoring. In September of 1983 the first satellite of the Russian *Okean-01* series with SLR (side-looking radar) was launched and, as a result, almost immediately shipping support became more efficient.



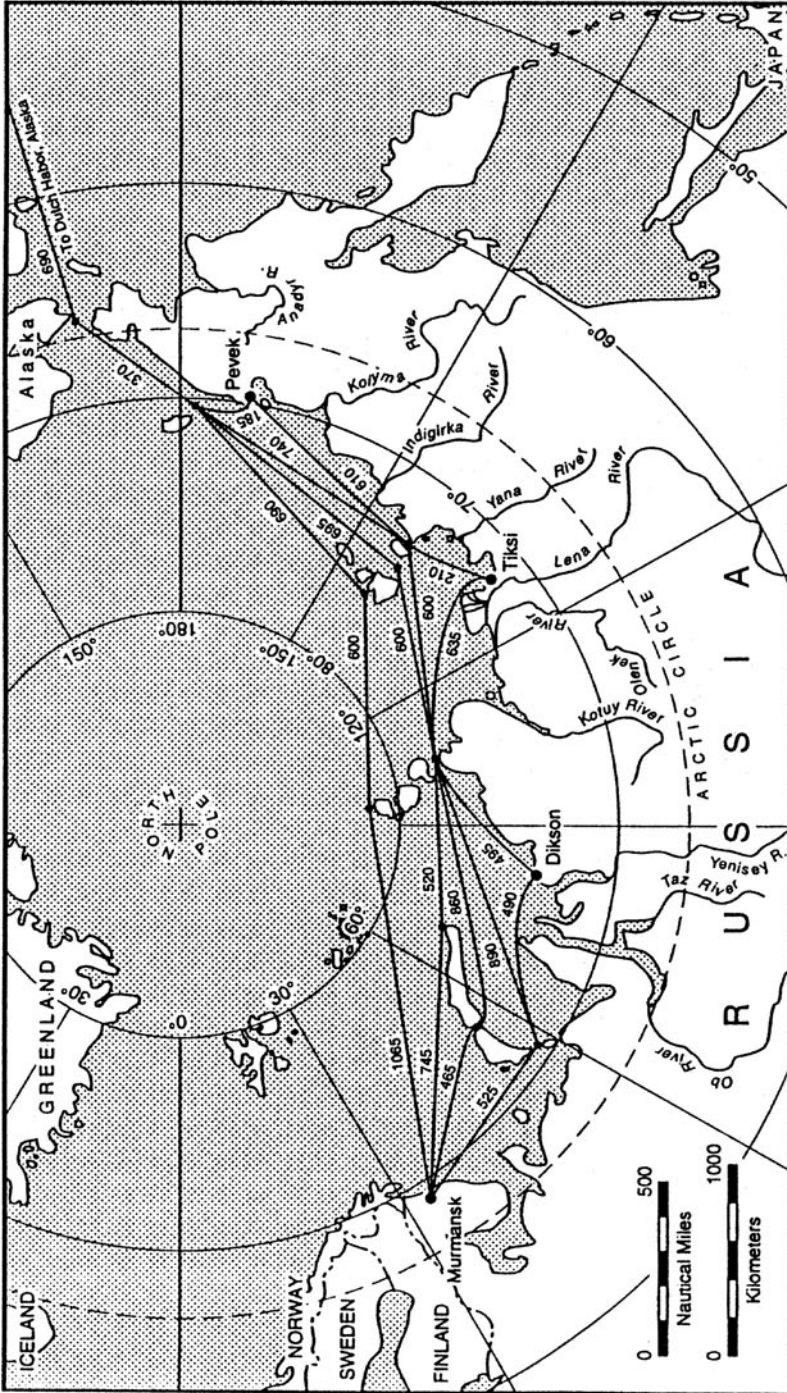


Figure 1. The major sailing routes along the NSR and distances between different sections in nautical miles.

Routine sea ice monitoring today is primarily based on satellite remote-sensing data in the optical and infrared range. However, weather- and light-independent satellite remote-sensing data in the microwave range significantly improved the availability of sea ice information. This began in the NSR in August 1991, just 2 weeks after the launch of the European Space Agency (ESA) *ERS-1* satellite, when real time synthetic aperture radar (SAR) images were transmitted to the French vessel *L'Astrolabe* to assist her navigation through the NSR from Europe to Japan. The *L'Astrolabe* expedition, headed by Pierre Sauvadet, included an *ERS-1* SAR project between ESA, with Guy Duchossois as *ERS-1* mission manager and the Nansen Environmental and Remote Sensing Center (NERSC) in Bergen, Norway, with Ola M. Johannessen as the project leader.

After the success of using SAR to route *L'Astrolabe* through the ice, the Nansen Centers in Bergen and St. Petersburg, and the Murmansk Shipping Company (MSC), conducted a number of campaigns to demonstrate the use of SAR for supporting the operations of the nuclear icebreakers of the MSC and their convoys. The principal project demonstrating the use of SAR in the NSR was “Icewatch” or, to give it its full title, “Real-Time Sea Ice Monitoring of the Northern Sea Route Using Satellite Radar Technology” that ran from 1994 to 1996. This was the first joint earth observation project between ESA and the Russian Space Agency (RKA). Partners in the “Icewatch Project”—in addition to ESA and RKA—were the Nansen Center in Bergen, the scientific and manufacturing association NPO Planeta and, later, the Scientific Research Centre for Exploration of Natural Resources (NITs IPR) in Moscow, the Arctic and Antarctic Research Institute (AARI) of Rosshydromet in St. Petersburg, the Scientific Foundation Nansen International Environmental and Remote Sensing Center in St. Petersburg and the Murmansk Shipping Company (MSC). Project leaders were Ola M. Johannessen of the Nansen Center and Alexey M. Volkov of the Scientific Research Center for Exploration of Natural Resources (NITs IPR) under RKA, with Guy Duchossois and Günther Kohlhammer of ESA and Georgy M. Polishuck of RKA as space agency representatives.<sup>1</sup> Based on the “Icewatch Project” two *ERS-1* and -2 SAR receiving stations were installed in the Russian Federation—one in Moscow and the other in Khantymaniisk in western Siberia.

Following on from the “Icewatch Project”, SAR data from *ERS-1* and -2, the Canadian *Radarsat* and the ESA *Envisat* started to be used semi-operationally in the NSR jointly with ice monitoring from AARI. This is the basis for this book, which is jointly written by authors from NERSC, AARI, NIERSC and MSC. Half of the writing of this book was funded by ESA through José Achache when he was Director of Earth Observation in ESA and Joseph Aschbacher, Programme Coordinator at ESA, while the remaining half was financed by institutional funding.

This book was also a component of the EU/INTAS Climate and Environmental Change in the Arctic (CECA) project, which was led by Prof. Ola M. Johannessen,

---

<sup>1</sup> Mr. Alain Fournier-Sicre, Head of the ESA Permanent Mission in the Russian Federation, Moscow, was instrumental in facilitating the cooperation between the two space agencies.

NERSC, with Dr. Leonid Bobylev, NIERSC, and Prof. Lennart Bengtsson, Max-Planck Institute for Meteorology, as partners. The CECA Project was awarded the Laureate of the EU transnational research Descartes Prize in Earth Science for 2005.

*Ola M. Johannessen*  
Director NERSC

*Leonid Bobylev*  
Director NIERSC

*Ivan Frolov*  
Director AARI

*Nina Novikova*  
NTsOMZ

*Volker Liebig*  
Director of EO, ESA

*Anatoly Eu. Shilov*  
Head of Department, RKA

## Acknowledgments

This book is based primarily on the joint research and demonstration projects carried out between 1991 and 2005. The first was the European Space Agency's (ESA) project "ERS-1 SAR Ice Routing of the *L'Astrolabe*" which supported the French vessel in her voyage through the Northern Sea Route in 1991. Subsequent projects were: the ESA-Norwegian Space Center's "ERS-1 Pilot Demonstration Project—Real-time Sea Ice Monitoring of the Northern Sea Route Using ERS-1 Satellite Radar Images" (1992–1995); the Nansen Center in Bergen's "SAR Strategy Program" (1994–1996) funded by the Research Council of Norway; ice routing of the Japanese project "*Kandalaksha '95 Voyage*" through the Northern Sea Route; the ESA-Russian Space Agency's (RKA) "Real-time Sea Ice Monitoring of the Northern Sea Route Using Satellite Radar Technology—Icewatch Project" (1994–1996); the three EU projects "Ice Routes" (1997–1998), "Arctic Demonstration and Exploratory Voyage—ARCDEV" (1998–1999) and the "Integrated Use of New Microwave Satellite Data for Improved Sea Ice Observations—IMSI" project (1997–1999); as well as the ESA GMES project "SAR Ice Monitoring for Climate Research—ICEMON" (2003–2005).

The authors acknowledge financial support of these projects given by these agencies and contributions from the many personnel who took part in these projects. We are especially grateful to the Murmansk Shipping Company (MSC), which has been, and still is, a close partner throughout these years. Of particular importance has been the support from Mr. Yu.F. Glushko and Mr. A.G. Gorshkovsky, Chiefs of MSC's nuclear icebreaker fleet. We appreciate cooperation in the field of the captains, ice pilots and crew of the MSC icebreakers *Sovetsky Soyuz*, *Yamal*, *Taymyr*, *Vaygach* and *Kapitan Dranitsyn*. We are also thankful to the Russian Ice Monitoring Service: in particular, hydrologist V.E. Pashchenko, Captain A.V. Smirnov, hydrologist A.Ya. Winter; Chief of the Marine Operational Headquarters (MOH) Mr. B. Berdnikov and Chief of the Science Operational Group (SOG) Dr. N. Adamovich, both located in Dikson.

xiv **Acknowledgments**

Studies with objectives of determining ice conditions in Arctic seas and developing methods for satellite information processing and analysis were carried out within the framework of these projects with the financial support of the Federal Service for Hydrometeorology and Environmental Monitoring and the Ministry of Education and Science of the Russian Federation. The authors are especially thankful to Professor A.V. Bushuyev, lead scientist in methods of sea ice remote sensing and Professor Z.M. Gudkovich, lead scientist in ice regime research at the Arctic and Antarctic Research Institute.

*The Authors*

# Figures

1.1	Map of the Arctic by Gerhardus Mercator (1512–1594) . . . . .	3
1.2	Map of the northern coast of Russia made by Isaac Massa in 1611 . . . . .	4
1.3	Eastward advances of the Russians in Northeast Asia in the 17th century . . .	5
1.4	The route of the first through-sailing in the Northern Sea Route by Nordenskjöld onboard <i>Vega</i> . . . . .	10
1.5	The map of the Arctic Ocean published by the <i>Petermans Geographische Mitteilungen</i> (Germany) in 1869 . . . . .	11
1.6	<i>Maud</i> 's route under sail and engine: the drifts of <i>Fram</i> , <i>Janette</i> and <i>Karluk</i> are also shown . . . . .	15
1.7	Map of the Northern Sea Route with the main transit routes (see also color section). . . . .	22
2.1	Annual variations in average drift velocity module . . . . .	33
2.2	Vectors of the average monthly drift velocity and dispersion ellipses . . . . .	33
2.3	Patterns of mean ice drift. . . . .	34
2.4	Fields of ice drift velocity in the Arctic Basin. . . . .	38
2.5	Probability of multi-year ice presence in the Arctic Basin . . . . .	40
2.6	Ice thickness distribution in the Arctic Basin . . . . .	42
2.7	The Arctic Eurasian Shelf seas and their regions . . . . .	45
2.8	Average dates of stable ice formation in Arctic seas . . . . .	47
2.9	Standard deviations of dates of stable ice formation in Arctic seas . . . . .	49
2.10	Changes in calculated mean multi-year ice thickness. . . . .	50
2.11	Calculated average and extreme landfast ice thickness . . . . .	51
2.12	Average distribution of ice of different age in Arctic seas at the end of the ice cover freezing period (see also color section) . . . . .	53
2.13	Mean multi-year values of seasonal changes in calculated ice exchange of the Kara and Laptev Seas with the Arctic Basin . . . . .	56
2.14	Location of landfast ice and flaw polynyas in the Arctic seas of the Siberian Shelf	58
2.15	Distribution of ice of different concentration in June (with a probability of 50%) (see also color section). . . . .	63

<b>2.16</b>	Distribution of ice of different concentration in July (with a probability of 50%) (see also color section) . . . . .	64
<b>2.17</b>	Distribution of ice of different concentration in August (with a probability of 50%) (see also color section) . . . . .	64
<b>2.18</b>	Distribution of residual ice of different concentration in September (with a probability of 50%) (see also color section) . . . . .	64
<b>3.1</b>	An example of the operational ice distribution chart in winter. . . . .	71
<b>3.2</b>	Aerial photo made by a circular plan-perspective AFC in the Lena River delta during the spring flood period (May 1968). . . . .	76
<b>3.3</b>	Study of the accuracy of laser aero-profilograms . . . . .	78
<b>3.4</b>	Ice reconnaissance aircraft <i>AN-24T</i> equipped with SLAR Toros . . . . .	80
<b>3.5</b>	Radar image and a photograph of one and the same sea ice area in autumn . . . . .	81
<b>3.6</b>	Radar image and a photograph of one and the same sea ice area in summer . . . . .	82
<b>3.7</b>	Remote ice reconnaissance <i>IL-24N</i> aircraft equipped with the radar system Nit'-C; and panel of on-line depiction of radar images and control of the Nit'-C system onboard <i>IL-24N</i> . . . . .	87
<b>3.8</b>	Standard layout of airborne ice observation routes. . . . .	88
<b>3.9</b>	Diagram of the earth's surface coverage by <i>Okean</i> sensors . . . . .	93
<b>3.10</b>	Example for the Kara Sea of superimposed images of the <i>Okean</i> satellite for 14 August 2000 . . . . .	94
<b>3.11</b>	Coverage of the NSR by <i>Okean-01</i> SLR images by 11 successive orbits . . . . .	94
<b>3.12</b>	<i>Okean</i> radar image (November, 1988) covering the area between Novaya Zemlya and Franz Josef Land . . . . .	96
<b>3.13</b>	Example of simultaneous <i>Okean</i> sea ice images during winter (January 1988) and summer (August 1988) . . . . .	97
<b>3.14</b>	Examples of daily and weekly operational ice charts (see also color section). . . . .	98
<b>3.15</b>	A sub-image of an <i>Almaz-1</i> SAR image from the Kara Gate . . . . .	103
<b>3.16</b>	Modes of operation of contemporary SAR systems (see also color section) . . . . .	105
<b>3.17</b>	Example of <i>Envisat</i> A-SAR images with alternating polarization . . . . .	108
<b>3.18</b>	<i>Envisat</i> A-SAR regional global mode mosaic in the Svalbard area on 11 May 2004 at 1-km resolution . . . . .	109
<b>3.19</b>	Examples of ice concentration maps in the Northern Sea Route (see also color section). . . . .	110
<b>3.20</b>	Examples of sea ice products obtained by passive microwave radiometer data . . . . .	114
<b>3.21</b>	Comparison of ice drift patterns in the Laptev Sea during 10–30 January 1998 . . . . .	116
<b>3.22</b>	The receiving zones over the Arctic from meteorological satellites of <i>NOAA</i> and <i>Terra</i> series covered by Russian stations . . . . .	117
<b>3.23</b>	Example of a weekly ice chart posted at AARI's Internet site (see also color section). . . . .	119
<b>3.24</b>	Weekly ice charts of the Kara Sea (see also color section). . . . .	120
<b>3.25</b>	Forecast of mean daily drift of sea ice. . . . .	122
<b>3.26</b>	Map resulting from tactical sea ice reconnaissance . . . . .	132
<b>3.27</b>	Countries with national ice services in the northern hemisphere (see also color section). . . . .	137
<b>3.28</b>	Example of regional ice chart for the southwestern Kara Sea from the U.S. National Ice Center (see also color section) . . . . .	141
<b>3.29</b>	Ice chart of the western Canadian Arctic from the Canadian Ice Service (see also color section) . . . . .	142

3.30	Example of weekly ice chart for Greenland waters from the Danish Meteorological Institute . . . . .	144
3.31	Example of ice chart from the Icelandic Ice Service . . . . .	146
3.32	Example of ice and sea surface temperature map from met.no (see also color section). . . . .	147
4.1	Spherical triangles solved in the geolocation process. . . . .	153
4.2	Example of a photo-chart from <i>NOAA</i> AVHRR after correction of geolocation by the coastline. . . . .	154
4.3	Example of a photo-chart from <i>NOAA</i> AVHRR in Mercator projection . . . .	156
4.4	Example of a composite photo-chart made by four <i>NOAA</i> AVHRR images. .	157
4.5	<i>NOAA</i> AVHRR visible and infrared images . . . . .	159
4.6	<i>NOAA</i> AVHRR optical images of sea ice in the Tatar Strait . . . . .	161
4.7	Example of ice thickness in the Barents Sea derived from <i>NOAA</i> AVHRR (see also color section). . . . .	170
4.8	Chart of ice thickness distribution in the Kara Sea. . . . .	171
4.9	The geometry of the satellite SAR system . . . . .	174
4.10	Scattering of electromagnetic waves of high- and low-frequency bands from smooth, rough and very rough surfaces. . . . .	176
4.11	The backscatter coefficient at C-band as a function of incidence angle for two major ice types and water during winter and summer. . . . .	181
4.12	Changes in <i>ERS</i> SAR backscatter of different types of sea ice. . . . .	185
4.13	SAR backscatter as a function of ice types . . . . .	189
4.14	The annual cycle of evolution of <i>ERS</i> SAR-derived backscatter for thick first-year ice and multi-year sea ice . . . . .	190
4.15	Photo of the effect of grease ice on damping of short wind waves . . . . .	193
4.16	Photo of grease ice observed in the ice edge region; and sub-image of an <i>ERS-1</i> SAR scene covering about 50 × 50 km from the marginal ice zone . . . . .	194
4.17	Photo of nilas after pressuring, causing formation of rafting and small ridges; and SAR image of smooth nilas . . . . .	196
4.18	Photo of gray ice with rough surface with many small edges. . . . .	197
4.19	Full-resolution ScanSAR sub-image with gray–white ice. . . . .	198
4.20	<i>Radarsat</i> ScanSAR wide image showing old ice . . . . .	199
4.21	<i>Envisat</i> ASAR image covering sea ice westward of Svalbard . . . . .	200
4.22	<i>Envisat</i> ASAR image showing winter sea ice conditions in the Kara Sea . . . .	201
4.23	Photo of pancake ice as often observed at the ice edge; <i>ERS</i> SAR signature of pancake ice interleaved with open water and grease ice. . . . .	203
4.24	<i>ERS-1</i> SAR scene covering Hopen Island, east of Svalbard. . . . .	204
4.25	Aerial photo of an 8 × 15 km area in transition between the interior of the pack ice and an intermediate zone . . . . .	205
4.26	<i>ERS-2</i> SAR image of western Vilkitskiy Strait and parts of Shokalskiy Strait .	206
4.27	Aerial photo covering an 8- × 8-km area of the ice edge region taken a few hours after an <i>ERS-1</i> overpass . . . . .	207
4.28	<i>ERS-1</i> SAR images every 3 days from the same descending path in the western Barents Sea. . . . .	208
4.29	<i>Radarsat</i> ScanSAR image covering the Pechora Sea . . . . .	210
4.30	<i>ERS-1</i> SAR image covering sea ice to the west of Yamal coast . . . . .	211
4.31	Full-resolution <i>Radarsat</i> ScanSAR wide image with icebreaker track . . . . .	213
4.32	<i>Radarsat</i> ScanSAR narrow image covering the northern part of the Gulf of Bothnia . . . . .	214



<b>4.33</b>	Annotated <i>Envisat</i> ASAR image covering the Kara Gate . . . . .	215
<b>4.34</b>	<i>ERS-2</i> SAR image covering the eastern part of Severnaya Zemlya . . . . .	217
<b>4.35</b>	Full-resolution <i>Radarsat</i> ScanSAR wide sub-image covering the western part of the Laptev Sea . . . . .	218
<b>4.36</b>	<i>ERS-2</i> SAR image covering outlet glaciers in the northern part of Novaya Zemlya. . . . .	219
<b>4.37</b>	Examples of sea ice segmentation of an <i>ERS</i> SAR image (see also color section)	225
<b>4.38</b>	Examples of MLP based sea ice classification of <i>Radarsat</i> ScanSAR images over the Kara and Barents Seas (see also color section) . . . . .	231
<b>4.39</b>	Ice concentration analysis from SAR and SSM/I images (see also color section)	237
<b>4.40</b>	Sequence of procedures for ice concentration retrieval from <i>Radarsat</i> image .	239
<b>4.41</b>	Ice motion in the Ob' River estuary computed from consecutive <i>ERS-1</i> SAR images . . . . .	242
<b>4.42</b>	Example of the working window used in interactive ice mapping in the GIS ArcView environment . . . . .	245
<b>4.43</b>	Examples of ice charts compiled from visible satellite images (see also color section). . . . .	247
<b>4.44</b>	Examples of ice charts compiled from satellite SAR images (see also color section). . . . .	250
<b>5.1</b>	Mean annual location of ice edge in the eastern Barents Sea and the southwestern Kara Sea during ice growth and decay . . . . .	255
<b>5.2</b>	Seasonal variability of ice edge position and its standard deviation at typical longitudes. . . . .	256
<b>5.3</b>	Variability of the close ice fraction in Kara Sea regions . . . . .	257
<b>5.4</b>	Frequency of close ice occurrence in the Novozemelsky ice massif. . . . .	259
<b>5.5</b>	Typical partitions of close ice areas in the Ob'–Yenisey and Yamalo–Yugorsky regions . . . . .	260
<b>5.6</b>	Typical partition of close ice in Severozemelsky ice massif regions . . . . .	261
<b>5.7</b>	Frequency of occurrence of close ice in the Severozemelsky ice massif in early August . . . . .	262
<b>5.8</b>	Typical partition of close ice in Severozemelsky ice massif regions . . . . .	263
<b>5.9</b>	The average extent of fast ice during its development near the Yamal Peninsula shore . . . . .	265
<b>5.10</b>	Diagram of smallest and greatest fast ice boundaries in the southeastern Barents Sea. . . . .	266
<b>5.11</b>	Satellite TV image of the northeastern part of the Kara Sea . . . . .	268
<b>5.12</b>	Average position of fast ice boundaries in the Kara Sea during the period of its growth . . . . .	269
<b>5.13</b>	Satellite TV images of the southwestern part of the Kara Sea . . . . .	271
<b>5.14</b>	<i>NOAA</i> AVHRR image showing leads in Kara Sea ice . . . . .	275
<b>5.15</b>	Estimates of specific length of leads for the Kara Sea . . . . .	277
<b>5.16</b>	Modal orientation of leads for the Kara Sea . . . . .	279
<b>5.17</b>	Average ice edge location in eastern Arctic seas . . . . .	282
<b>5.18</b>	Changes in standard deviations of ice edge location in the Laptev, East Siberian and Chukchi Seas . . . . .	283
<b>5.19</b>	The location of ice massifs in the eastern part of the Northern Sea Route . . .	284
<b>5.20</b>	Average fraction of ice massifs at the eastern segment of the Northern Sea Route during the period of melting. . . . .	285

5.21	Distribution of ice drift velocity in July–August in open areas of the southeastern Laptev Sea . . . . .	288
5.22	Temporal variability in average and extreme ice drift velocities in July–August 1986 in the southeastern Laptev Sea . . . . .	288
5.23	Distribution of ice drift velocity in the East Siberian Sea . . . . .	289
5.24	Satellite TV image of the eastern Laptev Sea and the western East Siberian Sea . . . . .	291
5.25	Average location of fast ice boundaries during the period of its growth in the Laptev Sea . . . . .	292
5.26	Average location of fast ice boundaries during the period of its growth in the East Siberian Sea . . . . .	294
5.27	Location of fast ice boundaries in the East Siberian Sea during its decay . . . . .	296
5.28	Average location of fast ice boundaries in the Chukchi Sea during its growth season . . . . .	297
5.29	Extent of fast ice in the western part of the Eurasian Arctic derived from <i>Radarsat</i> ScanSAR images . . . . .	303
5.30	<i>Radarsat</i> ScanSAR image showing fast ice in the eastern part of the Kara Sea more than 200 km out from the Yamal coast . . . . .	304
5.31	Example of <i>Radarsat</i> ScanSAR image for Franz Josef Land . . . . .	305
5.32	Franz Josef Land fast ice extent in March as derived from <i>Radarsat</i> images . . . . .	307
5.33	A series of four radar images covering the polynya at Cape Zhelaniya of Novaya Zemlya . . . . .	308
5.34	<i>Radarsat</i> ScanSAR images of polynyas near Novaya Zemlya . . . . .	311
5.35	Ice drift in the Laptev Sea in August–September 1997 derived from <i>Radarsat</i> images (see also color section) . . . . .	314
5.36	Patterns of scaled ice drift speed in the Laptev Sea derived from successive <i>Okean</i> RAR images during the winter of 1987/1988 . . . . .	316
5.37	Detailed ice drift trajectories of selected ice floes in the Laptev Sea, measured from successive <i>Okean</i> images over several months (see also color section) . . . . .	318
5.38	Vectors of scaled ice drift speed in the Laptev Sea from November to March, derived from successive <i>Okean</i> RAR and <i>Radarsat</i> ScanSAR images . . . . .	319
5.39	Vectors of scaled ice drift speed in the Laptev Sea from November to May from successive <i>Okean</i> RAR images . . . . .	322
6.1	Coverage of SAR images from ascending orbits of <i>ERS-1</i> between Dikson and Cape Chelyuskin during the <i>L’Astrolabe</i> voyage . . . . .	326
6.2	Communication lines during the voyage of <i>L’Astrolabe</i> through the Northern Sea Route . . . . .	327
6.3	SAR images acquired during the voyage of <i>L’Astrolabe</i> between Dikson and Cape Chelyuskin . . . . .	328
6.4	Track of the icebreaker <i>Sovetsky Soyuz</i> in November 1993 . . . . .	332
6.5	<i>ERS-1</i> SAR images with annotation of the main ice features during winter 1993 (see also color section) . . . . .	334
6.6	Annotated <i>ERS-1</i> SAR images during the <i>Vaygach</i> voyage in February–March 1994 . . . . .	340
6.7	<i>ERS-1</i> SAR image showing extensive ice cover in the western entrance to Vilkitsky Strait on 9 September 1994 . . . . .	344
6.8	Route taken by the <i>Kandalaksha</i> , the main ice edge location and areas selected for SAR acquisition . . . . .	345
6.9	Annotated <i>ERS</i> SAR image covering the area northwards of Severnaya Zemlya . . . . .	346

<b>6.10</b>	<i>ERS-1</i> SAR image transmitted in near-real time to the icebreaker <i>Vaygach</i> in the area west of Dikson on 26 January 1996 . . . . .	348
<b>6.11</b>	Subsets of <i>Radarsat</i> ScanSAR images showing the area east of Vilkitsky Strait (see also color section). . . . .	349
<b>6.12</b>	Photos of different ice conditions observed by the icebreaker <i>Sovetsky Soyuz</i> on 10–11 September within the SAR image of 7 September 7. . . . .	351
<b>6.13</b>	Mosaic of six ScanSAR images covering the Kara Sea during April–May 1998 . . . . .	353
<b>6.14</b>	<i>ERS-2</i> SAR image covering the Ob’ estuary . . . . .	355
<b>6.15</b>	Annotated <i>Envisat</i> ASAR scenes of the Kara Sea. . . . .	356
<b>6.16</b>	<i>Envisat</i> ASAR images in the Kara Sea during winter–spring 2004 . . . . .	360
<b>6.17</b>	Examples of <i>Envisat</i> ASAR images in the central part of the Kara Sea during the melt season of 2004. . . . .	363
<b>6.18</b>	Mosaic of <i>Envisat</i> ASAR images for the Pechora and Kara Seas for 26–28 February 2005 with overlaid route of convoy. . . . .	366
<b>6.19</b>	Mosaic of <i>Envisat</i> ASAR images for the Pechora and Kara Seas for 21–24 May 2005. . . . .	367
<b>6.20</b>	<i>Meteor-3</i> and <i>-5</i> images of the Kara Sea . . . . .	375
<b>6.21</b>	Example of a combined depiction of the <i>NOAA</i> raster image and the navigation chart in ECDIS (see also color section) . . . . .	376
<b>6.22</b>	Icebreaker forcing orthogonal to the front of ice pressure. . . . .	378
<b>6.23</b>	Relative increase in mean convoy routing speed in the ice as a function of the resolution of ice information . . . . .	379
<b>6.24</b>	Speed of convoys routed by <i>Arktika</i> -type icebreakers for different ice thickness . . . . .	379
<b>6.25</b>	Seasonal change in mean speed of convoys when using tactical ice reconnaissance data or not (see also color section) . . . . .	380
<b>6.26</b>	Example of ice drift and deformation of a grid cell observed in a sequence of SAR images . . . . .	383
<b>6.27</b>	Sea ice vorticity and shear fields calculated from 6-day interval mosaics (see also color section) . . . . .	384
<b>6.28</b>	Examples of ice ridge mapping in the Gulf of Bothnia . . . . .	385
<b>6.29</b>	Sea ice freeboard from one 35 day cycle of <i>ERS</i> radar altimeter data; and ice thickness map from the Beaufort Sea (see also color section). . . . .	386
<b>6.30</b>	Ice surface height from <i>IceSat</i> (see also color section) . . . . .	387
<b>6.31</b>	Example of profile of ice thickness and surface height derived from electromagnetic induction measurements from helicopter flights . . . . .	388
<b>6.32</b>	Ice freeboard image from scanning laser; and same area observed by a vertical video camera (see also color section). . . . .	389
<b>6.33</b>	Illustration of an upward-looking sonar mooring deployed under the ice; and map of ULS moorings deployed in various parts of the Arctic Ocean . . . . .	389
<b>6.34</b>	Location and drift trajectories for IABP buoys in operation in September 2005 . . . . .	390
<b>6.35</b>	GPR section (radargram) obtained from a sled covering a distance of 200 m on a multi-year ice floe north of Svalbard (see also color section) . . . . .	391
<b>6.36</b>	Example of comparison between EM draft data from helicopter and ground penetrating draft data from a sled (see also color section) . . . . .	391
<b>6.37</b>	Example of combined interpretation of SAR and optical satellite images . . . . .	393
<b>6.38</b>	Sea ice classification maps obtained from satellite images (see also color section) . . . . .	395
<b>7.1</b>	Linear trends of ice extent in the western and eastern Arctic seas over the period 1900–2003 (August). . . . .	400
<b>7.2</b>	Linear trend of ice extent in the Beaufort Sea in August from 1968 to 1998 . . . . .	401

<b>7.3</b>	Linear trends of total ice extent in August over the periods 1900–1945 and 1946–2003 in western and eastern Arctic seas . . . . .	401
<b>7.4</b>	Functions of the spectral density of total ice extents in August in western and in eastern Arctic seas. . . . .	404
<b>7.5</b>	Anomalies of mean annual air temperature in the Arctic zone from 1900 to 2003	405
<b>7.6</b>	Fluctuations in total ice extent in various Arctic seas . . . . .	406
<b>7.7</b>	Arctic sea ice area derived from satellite passive microwave sensor data, 1978–2005. . . . .	410
<b>7.8</b>	Mean sea ice concentration in the Arctic derived from satellite passive microwave sensor data, 1978–2005, in winter and summer (see also color section) . . . . .	411
<b>7.9</b>	Linear trend for Arctic sea ice area anomalies derived from satellite passive microwave sensor data, 1978–2005 . . . . .	412
<b>7.10</b>	Linear trends in Arctic sea ice concentration derived from satellite passive microwave sensor data, 1978–2005, in winter and summer (see also color section)	413
<b>7.11</b>	Arctic summer minimum (mean for September month) for 2002–2005; an mean for September from 1979 to 2005 (see also color section) . . . . .	414
<b>7.12</b>	Arctic total sea ice concentration and its multi- and first-year components (see also color section) . . . . .	416
<b>7.13</b>	Variability and trends in winter multi-year ice area, mean of February and March from 1978 to 1998 . . . . .	417
<b>7.14</b>	Statistical model forecast of the climatic component of total ice extent in western and eastern Arctic seas for the 21st century relative to the linear trend . . . . .	419
<b>7.15</b>	HadCM3-modelled northern hemisphere sea ice concentrations in winter during this century (see also color section) . . . . .	420
<b>7.16</b>	Projected changes in navigation season for the Northern Sea Route in the 21st century based on five-model output (see also color section). . . . .	422

# Tables

<b>1.1</b>	Number of ships and volume of shipping along the Kara Sea Route in 1901–1919	13
<b>1.2</b>	Marine cargo transportation along the NSR 1945 to 1975	22
<b>2.1</b>	Estimates of average ice area in different regions of the northern hemisphere during the period of seasonal maximum and minimum	26
<b>2.2</b>	Estimates of average ice area in the marginal seas of the Arctic Ocean during the period of seasonal maximum and minimum	27
<b>2.3</b>	Estimates of the contribution of interannual ice area variability of individual regions to total interannual ice area variability of the Arctic Ocean	27
<b>2.4</b>	Estimates of ice volume in the Arctic Ocean and its large regions for the periods of seasonal maximum and minimum	28
<b>2.5</b>	Estimates of ice volume accounting for ridged ice features in the Arctic Ocean during periods of maximum and minimum ice cover development	29
<b>2.6</b>	Statistical ice drift characteristics averaged over a year for different periods	30
<b>2.7</b>	Values of the distribution function parameters of ice drift velocity modules depending on the period of averaging of the resulting speed	31
<b>2.8</b>	Frequency of occurrence of types of structures in the ice drift field in the Arctic Basin, 1979–2002	39
<b>2.9</b>	Estimates of mean weighted ice thickness distribution in the Arctic Basin during the spring period	43
<b>2.10</b>	Time of onset of main ice melting stages in the Arctic Basin	43
<b>2.11</b>	Ice melting value at different multi-year ice relief features	44
<b>2.12</b>	Average ice thickness growth rate in Arctic seas based on data from polar stations	48
<b>2.13</b>	Ice age composition in regions of the Arctic seas in autumn–winter periods	52
<b>2.14</b>	Ice age composition in autumn–winter periods in the Barents Sea regions	53
<b>2.15</b>	Average and maximal areas of landfast ice in regions of the Arctic seas from 1949 to 2002	59
<b>2.16</b>	Mean multi-year characteristics of flaw polynyas in Arctic seas from November to June	61

<b>2.17</b>	Mean multi-year characteristics of flaw polynyas of Franz Josef Land in February to May. . . . .	61
<b>2.18</b>	Area of ice-free regions in Arctic seas during the period of melting . . . . .	63
<b>3.1</b>	Main characteristics of instrumentation of satellite <i>Okean-01</i> . . . . .	92
<b>3.2</b>	Parameters of SAR system mounted onboard <i>Seasat</i> and <i>Space Shuttles</i> . . . .	102
<b>3.3</b>	Parameters of <i>Almaz-1</i> SAR. . . . .	102
<b>3.4</b>	Parameters of <i>ERS-1/2</i> SAR . . . . .	104
<b>3.5</b>	Parameters of <i>Radarsat-1</i> and <i>Radarsat-2</i> SAR . . . . .	106
<b>3.6</b>	Parameters of <i>Envisat</i> ASAR . . . . .	107
<b>3.7</b>	Emissivities of water and ice. . . . .	111
<b>3.8</b>	Parameters of satellite passive microwave sensors. . . . .	112
<b>3.9</b>	World Wide Web addresses of the main ice services in the northern hemisphere	148
<b>4.1</b>	Spectral ranges and resolution of MODIS channels . . . . .	151
<b>4.2</b>	Accuracy of sea ice characteristic determination from optical satellite images .	164
<b>4.3</b>	Comparison of sea ice thickness determined from an IR image and onboard ships	170
<b>4.4</b>	Comparison of sea ice thicknesses determined from an IR image and at coastal stations . . . . .	172
<b>4.5</b>	Symbols for electromagnetic wavelength bands used in radar remote sensing .	175
<b>4.6</b>	Description of ice classes and the number of training and test feature vectors for each class . . . . .	228
<b>4.7</b>	Backscatter contrast between calm open water and sea ice for <i>ERS-1</i> SAR . .	234
<b>5.1</b>	Mean and extreme areas of fast ice during the period of growth in the Kara Sea from satellite data from 1980 to 2002 . . . . .	270
<b>5.2</b>	Mean frequency of occurrence and characteristics of polynyas of the Kara Sea from satellite data from November to June 1979–2003 . . . . .	273
<b>5.3</b>	Mean monthly frequency of occurrence of polynyas in the Kara Sea observed from satellite data from 1979 to 2003 . . . . .	273
<b>5.4</b>	Inter-annual variability in frequency of occurrence of polynyas in the Kara Sea observed from satellite data from 1979 to 2003 . . . . .	274
<b>5.5</b>	Monthly mean and maximum specific lengths of leads (discontinuities) in the ice cover of the Kara Sea . . . . .	278
<b>5.6</b>	Mean and maximum lengths of leads (discontinuities) in the ice cover of the Kara Sea. . . . .	280
<b>5.7</b>	Ice-free area during each summer month in different regions of eastern Eurasian Arctic seas . . . . .	281
<b>5.8</b>	Occurrence of complete disappearance of ice massifs from 1973 to 2003. . . .	285
<b>5.9</b>	Mean and extreme areas of ice massifs and their standard deviations for 1973–2003. . . . .	286
<b>5.10</b>	Statistical characteristics of ice drift speed in the East Siberian Sea . . . . .	290
<b>5.11</b>	Statistical characteristics of ice drift speed in the East Siberian Sea . . . . .	290
<b>5.12</b>	Mean and extreme fast ice areas during the period of growth in the Laptev Sea based on satellite data from 1980 to 2002 . . . . .	293
<b>5.13</b>	Mean and extreme fast ice areas during the period of growth in the East Siberian Sea based on satellite data from 1980 to 2002 . . . . .	295
<b>5.14</b>	Mean and extreme fast ice areas during the period of growth in the southwestern Chukchi Sea in the middle of the month from satellite data from 1980 to 2003	297
<b>5.15</b>	Mean frequency of occurrence and characteristics of polynyas of the Eastern Arctic Seas from satellite data from November to June 1979–2003 . . . . .	298

<b>5.16</b>	Mean monthly frequency of occurrence of polynyas of the eastern Eurasian Arctic Seas from satellite data from 1979 to 2003. . . . .	299
<b>5.17</b>	Annual variability in frequency of occurrence of polynyas of eastern Arctic seas from satellite data from 1979 to 2003 . . . . .	300
<b>5.18</b>	Mean and standard deviation of polynya widths as determined from SAR images	312
<b>6.1</b>	SAR sea ice demonstration campaigns in the Northern Sea Route. . . . .	324
<b>6.2</b>	Number of received <i>ERS-1</i> SAR images/orbital passes during the 1993 demonstration campaign . . . . .	333
<b>6.3</b>	Summary of satellite SAR systems . . . . .	382
<b>7.1</b>	Contribution of climatic components to total variance in fluctuations of total ice extent in different Arctic regions. . . . .	407
<b>G.1</b>	Total concentration of ice . . . . .	432
<b>G.2</b>	Stage of development and thickness . . . . .	432
<b>G.3</b>	Form of ice . . . . .	433

# Abbreviations

AARI	Arctic and Antarctic Research Institute
ACIA	Arctic Climate Impact Assessment
AFC	Aerial photo camera
AIISA	Automated Ice Information System for the Arctic
AIJEX	Arctic Ice Joint Experiment Study
AIRP	Automated Information Receiving Point
AMSR	Advanced Microwave Scanning Radiometer
ANSR	Administration of the Northern Sea Route
AO	Arctic Oscillation
AP	Alternating Polarization
APT	Automatic Picture Transmission
ARCDEV	ARCTic Demonstration and Exploratory Voyage
ARGOS	Satellite-based location and environmental data collection system
ARI	Arctic Research Institute
ARKTOS	Advanced system for classification of sea ice types in satellite radar images
ARO	Arctic Research Observatory
ASAR	Advanced SAR
ASF	Alaska SAR Facility
AVHRR	129, 149–150
BMP	Windows BitMaM
CCG	Canadian Coast Guard
CIHMI	Center for Ice and Hydrometeorological Information
CIM	Composite Ice Map
CIS	Canadian Ice Service
CNSR	Committee of the Northern Sea Route
DARMS	Drifting Automatic Radio Meteorological Stations



DMI	Danish Meteorological Institute
DMSP	Defense Meteorological Satellite Program
DN	Digital Number
ECDIS	Electronic Chart Display and Information System
ECHAM-4	Max-Planck Institute for Meteorology in Hamburg, Germany
ECNIS	Electronic Cartographic Navigation Information System
EEA	Exclusive Economic Area
EM	ElectroMagnetic
EO	Earth Observation
EOS	Earth Observation System
ERS	European Remote Sensing satellite
ESA	European Space Agency
ESMR	Electrically Scanning Microwave Radiometer
ESTEC	European Space Research and TEChnology Centre of ESA
ETSI	Expert Team on Sea Ice
EU	European Union
EUMETSAT	EUropean organization for the exploration of METEorological SATellites
FNMOC	Fleet Numerical Meteorological and Oceanographic Center
FRI	Full-Resolution Image
FTP	File Transfer Protocol
FYI	First-Year Ice
GHG	GreenHouse Gas
GIF	Graphic Interchange Format
GIS	Geographical Information System
GLCM	Gray Level Co-occurrence Matrix
GLONAS	A global positioning system
GMES	Global Monitoring for Environment and Security
GMT	Greenwich Mean Time
GPR	Ground Penetrating Radar
GPS	Global Positioning System
HadCM3	Hadley Centre at the UK Met Office
HDF	Hierarchical Data Format
HF	High Frequency (radar)
HH	Horizontal polarization
HMS	HydroMeteorological Service
HRPT	High-Resolution Picture Transmission
HV	Transmission is made in one polarization and receiving in another
IABP	International Arctic Buoy Program
ICG	Icelandic Coast Guard
ID	IDentifier
IFREMER	French Research Institute for Exploitation of the Sea
IICWG	International Ice Charting Working Group

IIP	International Ice Patrol
IMO	Icelandic Meteorological Office
IPCC	Intergovernmental Panel on Climate Change
IR imager	InfraRed radiometer
IR	InfraRed
JPEG	Joint Photographic Expert Group (file format)
KSAT	Kongsberg SATellite Services, Tromsø, Norway
LDA	Linear Discriminant Analysis
LFO	Low-Frequency Oscillation
LKF	Linear Kinematic Feature
LNG	Liquefied Natural Gas
LRI	Low-Resolution Image
MANSR	Main Administration of the Northern Sea Route
MCC	Multiple Cross Correlation
met.no	Norwegian Meteorological Institute
MIZ	Marginal Ice Zone
MLP	Multi-Layer Perceptron
MMF	Ministry of Marine Fleet
MODIS	MODERate-resolution Imaging Spectroradiometer
MOH	Marine Operations Headquarters
MOS	Japanese Marine Observation Satellite
MSC	Meteorological Service of Canada
MSC	Murmansk Shipping Company
MYI	Multi-Year Ice
NAO	North Atlantic Oscillation
NASA	National Aeronautical and Space Administration
NAVICEEN	Naval Ice Center
NAVOCEANO	Naval Oceanographic Office
NCEP	National Center for Environmental Prediction
NERSC	Nansen Environmental and Remote Sensing Center
NESDIS	National Environmental Satellite Data Information Service
NIB	Nuclear IceBreaker
NIC	National Ice Center
NIERSC	Nansen International Environmental and Remote Sensing Centre
NOAA	National Oceanographic and Atmospheric Administration
NORSEX	NORwegian Remote Sensing EXperiment
NPI	Norwegian Polar Institute
NRT	Near-Real Time
NSIDC	National Snow and Ice Data Center
NSRA	NSR Administration
NZN	Novozemelsky northern ice massif
NZS	Novozemelsky southern ice massif
OY	Ob'–Yenisey
PAF	Processing and Archiving Facility (ESA)

PALSAR	Phased Array L-band Synthetic Aperture Radar
PDF	Probability Density Function
RAR	Real Aperture Radar
RGPS	<i>Radarsat</i> Geophysical Processor System
RICAE	Riga Institute of Civil Aviation Engineers
RKA	Russian Space Agency
RMS	Root Mean Square
RRMC	Regional Radio-Meteorological Center
RT	Real Time
SAR	Synthetic Aperture Radar
SAT	Surface Atmospheric Temperature
SLAR	Side-Looking Airborne Radar
SLP	Sea Level Pressure
SLR	Side-Looking Radar
SMMR	Scanning Multi-channel Microwave Radiometer
SRES	Special Report on Emission Scenarios
SSM/I	Special Sensor Microwave/Imager
SST	Sea Surface Temperature
SWK	SouthWestern Kara Sea (SWK)
SZE	Severozemelsky eastern ice massif
SZW	Severozemelsky western ice massif
TIFF	Tagged Image File Format
TM	Thematic Mapper
TSS	Tromsø Satellite Station (now KSAT)
UGMS	Yakutian Administration of the Hydrometeorological Service
UL, ULA	Classes of ice-strengthened ships
ULS	Upward-Looking Sonar
URL	Uniform Resource Locator
VH	Transmission is made in one polarization and receiving in another
VH	Vertical polarization
VPI	Russian system for broadcasting of information
WMF	Windows Meta File
WMO	World Meteorological Organization
WS	Wide-Swath
WSM	Wide-Swath radar Mode on <i>Envisat</i>
WWW	World Wide Web
YY	Yamalo–Yugorsky

# Authors

**Prof. Ola M. Johannessen**

Nansen Environmental and Remote Sensing Center,  
Mohn-Sverdrup Center for Global Ocean Studies and Operational Oceanography and  
Geophysical Institute, University of Bergen, Bergen, Norway  
*Ola.Johannessen@nersc.no*

**Dr. Vitaly Yu. Alexandrov**

Nansen International Environmental and Remote Sensing Centre, St. Petersburg, Russia  
*Vitali.Alexandrov@nersc.spb.ru*

**Prof. Ivan Ye. Frolov**

Arctic and Antarctic Research Institute, St. Petersburg, Russia  
*Frolov@aari.nw.ru*

**Prof. Stein Sandven**

Nansen Environmental and Remote Sensing Center, Bergen, Norway and  
University Courses on Svalbard—UNIS, Longyearbyen, Svalbard, Norway  
*Stein.Sandven@nersc.no*

**Mr. Lasse H. Pettersson**

Nansen Environmental and Remote Sensing Center, Bergen, Norway  
*lasse.pettersson@nersc.no*

**Dr. Leonid P. Bobylev**

Nansen International Environmental and Remote Sensing Centre, St. Petersburg, Russia and  
Nansen Environmental and Remote Sensing Center, Bergen, Norway  
*Leonid.Bobylev@nersc.spb.ru*

**Mr. Kjell Kloster**

Nansen Environmental and Remote Sensing Center, Bergen, Norway  
*Kjell.Kloster@nersc.no*

**Dr. Vladimir G. Smirnov**

Arctic and Antarctic Research Institute, St. Petersburg, Russia

*Vgs@aari.nw.ru*

**Dr. Yevgeny U. Mironov**

Arctic and Antarctic Research Institute, St. Petersburg, Russia

*Mir@aari.nw.ru*

**Mr. Nikolay G. Babich**

Murmansk Shipping Company, Murmansk, Russia

*Deyneka@msco.ru*

## Contributing authors

**Alexandrov, Vitaly Yu.**

Nansen International Environmental and Remote Sensing Centre, St. Petersburg, Russia  
*Vitali.Alexandrov@niersc.spb.ru*

**Babich, Nikolay G.**

Murmansk Shipping Company, Murmansk, Russia  
*Deyneka@msco.ru*

**Babiker, Mohamed**

Nansen Environmental and Remote Sensing Center, Bergen, Norway  
*Mohamed.Babiker@nersc.no*

**Bobylev, Leonid P.**

Nansen International Environmental and Remote Sensing Centre, St. Petersburg, Russia and  
Nansen Environmental and Remote Sensing Center, Bergen, Norway  
*Leonid.Bobylev@niersc.spb.ru*

**Bogdanov, Andrey V.**

Ruhr-Universitaet, Institut fuer Neuroinformatik, Bochum, Germany  
*Andrey.Bogdanov@neuroinformatik.ruhr-uni-bochum.de*

**Borodachev, Viktor Ye.**

Arctic and Antarctic Research Institute, St. Petersburg, Russia  
*Aaricoop@aari.nw.ru*

**Bushuev, Andrey V.**

Arctic and Antarctic Research Institute, St. Petersburg, Russia  
*Aaricoop@aari.nw.ru*

**Frolov, Ivan Ye.**

Arctic and Antarctic Research Institute, St. Petersburg, Russia

*Frolov@aari.nw.ru*

**Gorbunov, Yury A.**

Arctic and Antarctic Research Institute, St. Petersburg, Russia

*Gua@aari.nw.ru*

**Gudkovich, Zalman M.**

Arctic and Antarctic Research Institute, St. Petersburg, Russia

*Aaricoop@aari.nw.ru*

**Johannessen, Ola M.**

Nansen Environmental and Remote Sensing Center, Mohn-Sverdrup Center for Global Ocean Studies and Operational Oceanography and Geophysical Institute, University of Bergen, Bergen, Norway

*Ola.Johannessen@nersc.no*

**Karelin, Igor D.**

Arctic and Antarctic Research Institute, St. Petersburg, Russia

*Aaricoop@aari.nw.ru*

**Karklin, Valery P.**

Arctic and Antarctic Research Institute, St. Petersburg, Russia

*Karklin@aari.nw.ru*

**Kloster, Kjell**

Nansen Environmental and Remote Sensing Center, Bergen, Norway

*Kjell.Kloster@nersc.no*

**Losev, Stanislav M.**

Arctic and Antarctic Research Institute, St. Petersburg, Russia

*Aaricoop@aari.nw.ru*

**Loshchilov, Viktor S.**

Arctic and Antarctic Research Institute, St. Petersburg, Russia

*Lvs@aari.nw.ru*

**Lundhaug, Maria**

Nansen Environmental and Remote Sensing Center, Bergen, Norway

*Maria.Lundhaug@vesta.no* (current affiliation)

**Melentyev, Vladimir V.**

Nansen International Environmental and Remote Sensing Centre, St. Petersburg, Russia

*Vladimir.Melentyev@niersc.spb.ru*

**Miles, Martin**

Bjerknes Centre for Climate Research, Bergen, Norway and

University of Bergen, Bergen, Norway

*Martin.Miles@geo.uib.no*

**Mironov, Yevgeny U.**

Arctic and Antarctic Research Institute, St. Petersburg, Russia

*Mir@aari.nw.ru*

**Myrmehl, Cathrine**

Nansen Environmental and Remote Sensing Center, and

Mohn-Sverdrup Center for Global Ocean Studies and Operational Oceanography, Bergen, Norway

*Cathrine.Myrmehl@nersc.no*

**Paramonov, Alexandr I.**

Arctic and Antarctic Research Institute, St. Petersburg, Russia

*Paramonov@aari.nw.ru*

**Pettersson, Lasse H.**

Nansen Environmental and Remote Sensing Center, Bergen, Norway

*lasse.pettersson@nersc.no*

**Sandven, Stein**

Nansen Environmental and Remote Sensing Center, Bergen, Norway and

University Courses on Svalbard—UNIS, Longyearbyen, Svalbard, Norway

*Stein.Sandven@nersc.no*

**Shcherbakov, Yuriy A.**

Arctic and Antarctic Research Institute, St. Petersburg, Russia

*Jas@aari.nw.ru*

**Smirnov, Vladimir G.**

Arctic and Antarctic Research Institute, St. Petersburg, Russia

*Vgs@aari.nw.ru*

**Spichkin, Vladimir I.**

Arctic and Antarctic Research Institute, St. Petersburg, Russia

*Aaricoop@aari.nw.ru*

**Zaitsev, Lev V.**

Nansen International Environmental and Remote Sensing Centre, St. Petersburg, Russia

*Lev.Zaitsev@niersc.spb.ru*



# Introduction

This book covers a range of topics related to the monitoring of sea ice conditions in support of navigation in the Northern Sea Route (NSR). It includes the history of exploration of the Northern Sea Route, organization of sea ice monitoring, analysis of sea ice conditions, methodologies of satellite remote sensing of sea ice for supporting navigation and climatic variability of sea ice conditions in the Arctic Ocean and the Northern Sea Route. Use of the most advanced microwave techniques of sea ice monitoring—such as SAR data provided by the European *ERS-1*, *ERS-2*, *Envisat* and the Canadian *Radarsat* satellites—is specifically addressed.

**Chapter 1** presents a brief history of Northern Sea Route exploration, the present period and future prospects for its use. During the 17th century the Russian Pomors and Cossacks sailed along the western and eastern parts of the Northeast Passage and discovered the Bering Strait. In the early 18th century the Great Northern Expedition mapped almost the entire coast of the Arctic Ocean. Many renowned expeditions were accomplished in the 19th century. Thus, Nordenskjöld onboard *Vega* passed for the first time through the entire NSR. De-Long attempted to reach the North Pole onboard *Jeannette*. Fridtjof Nansen's *Fram* sailed eastward through the Kara and Laptev Seas, where her transarctic drift started. Also, from the second half of the 19th century, trade shipping was developed in the Kara Sea for exporting Siberian mineral resources and importing industrial goods. By the beginning of the 20th century the whole Arctic coast had been discovered and studied, and navigation maps of Eurasian Arctic seas produced.

Studies and exploration of the Northern Sea Route continued during the Soviet period using icebreakers, aircraft, research vessels and a network of hydrometeorological stations. In 1932 the Northern Sea Route Administration was given the task of finally laying out the sea route from the White Sea to the Bering Strait, equipping and maintaining it in good state and ensuring safe navigation along it. Accordingly, a service of hydrometeorological support including sea ice monitoring for navigation was organized. In 1933 the *Sibiriyakov* completed her voyage all along the NSR during

one navigation summer season. Since 1935, shipping operations—servicing the extensive industrial development in the Eurasian coastal Arctic area—were conducted according to the Soviet plan for cargo operations. Transport of goods in the Northern Sea Route continuously increased and during the late 1980s more than 6 million tons per year were shipped.

From July 1991 the NSR was officially declared open for non-Russian merchant vessels, and the French vessel *L'Astrolabe* was the first to pass through from west to east. However, after the Soviet period, much of the industrial production in the northern regions decreased and cargo turnover through the NSR was only 1.5–2.0 million tons after 1996.

However, the recent increase in oil and gas exploration and production and the associated increase in industrial activities in the areas of the far north of Russia will cause a further increase in transport in the NSR in the years to come, since the shelf area of the Arctic Ocean has 20–25% of the world's remaining oil and gas reserves. Therefore, safe operation in ice-infested waters in the NSR requires real time hydro-meteorological and sea ice information of high quality and reliability.

**Chapter 2** is devoted to sea ice conditions for the whole Arctic Ocean and in Eurasian Arctic Shelf seas. Significant seasonal changes in ice area in the Arctic Ocean occur in the marginal seas, with the seasonal maximum and minimum of ice extent in March–April and in September, respectively. Two major features of ice drift in the Arctic Ocean are the anticyclonic Beaufort Gyre and the transarctic ice flow between the North Pole and the northern margins of Eurasian Shelf seas, towards the Greenland Sea and Fram Strait.

Knowledge of sea ice conditions in Eurasian Arctic seas is essential for navigation in the Northern Sea Route and the offshore industry. Analysis of 50 years of observations from Russian polar stations and visual ice reconnaissance data allowed studying of ice formation and ice thickness growth, ice exchange between Eurasian Arctic seas and the Arctic Basin, distribution of fast ice, flaw polynyas and drifting ice. First-year ice prevails in Arctic Shelf seas; however, multi-year ice is often observed in the East Siberian Sea and in the northern parts of the Laptev and Kara Seas. On average, before the annual onset of ice formation, 80% of the eastern Laptev Sea and 85% of the southwestern Chukchi Sea are ice-free while the Barents Sea and the southwestern Kara Sea are almost ice-free. The northeastern Kara Sea and the western areas of the Laptev Sea and the East Siberian Sea become approximately 50% ice-free.

**Chapter 3** addresses various aspects of sea ice monitoring and services in the NSR and in other Arctic countries. Soviet sea ice reconnaissance flights were made part of the hydrometeorological service for navigation at the beginning of the 1930s, and later on ice reconnaissance flights were made every 10 days more or less regularly during the entire navigation period. In the last decades of the 20th century various airborne remote-sensing techniques—such as side-looking airborne radars, radar video-impulse sea ice thickness meter, optical and radar satellite images—were implemented and widely used for operational support of shipping and compilation of weekly composite ice charts for the entire NSR. The first stage of an automated ice information system for the Arctic was accepted for commercial operation in 1989.

The Center for Ice and Hydrometeorological Information at the Arctic and Antarctic Research Institute (AARI) provides ice information to users in near-real time. They regularly issue ice charts and ice forecasts. With the end of regular airborne ice reconnaissance in the early 1990s, satellites became the main tool for acquisition of sea ice information.

To ensure safe operations in ice-covered seas operational monitoring of sea ice and icebergs has been developed in Arctic countries over several decades. The major ice services in the northern hemisphere are the U.S. National Ice Service, the Canadian Ice Service, the Danish Ice Service for Greenland waters, the Icelandic Ice Service and the Norwegian Ice Service, all of which are briefly described.

A study of users' requirements for sea ice information was done as part of the "Icewatch Project". The major user of sea ice information for navigation in the NSR is the Murmansk Shipping Company, being responsible for provision of icebreaker escort of merchant ice class cargo vessels and tankers. Depending on the purpose, tasks and objectives, ice information is divided into three main categories: strategic, operational and tactical. Analysis of different remote-sensing data concludes that *Envisat* and *Radarsat* SAR radar images, which can cover the entire area of the NSR in a 48-hour period, to a large extent satisfy users' requirements for support of navigation in sea ice, and therefore need to be routinely implemented in AARI's operational systems.

**Chapter 4** deals with methodologies of satellite remote sensing of sea ice. Currently, Russian sea ice monitoring of the Northern Sea Route is based primarily on the optical and infrared images from *NOAA* and *Terra* satellites. Classification of sea ice parameters from these images is done, and derivation of ice thickness using IR images is also possible in the absence of clouds and for sea ice up to 120 cm thick.

The major principles of synthetic aperture radar (SAR) are described. Analysis of backscatter ( $\sigma^0$ ) from sea ice shows that, at the C-band, surface scattering is predominant for young and first-year ice, as well as summer ice, while volume scattering is typical of old ice in winter conditions. Typical changes in radar backscatter from sea ice during winter are: low backscatter from grease and new ice and nilas; increase for pancake and gray ice; decrease in first-year ice; and, finally, increase for multi-year ice. Significant differences between the backscatter of the same ice types was found between sea ice at the ice edge and within the pack ice, but this was due to different roughness.

Signatures of the principal sea ice types and their expressions in *ERS*, *Radarsat* and *Envisat* SAR images have been specified and verified based on a series of subsatellite field experiments. The main sea ice parameters—including stages of ice development, forms of fast ice and pack ice, ice edge location, polynyas, ice surface features and icebergs—have been derived from radar images. Some ambiguities in their interpretation are caused by the similarity of signatures between different sea ice types and features. Techniques currently used for automatic classification of SAR images are presented. Furthermore, description of the methodology of ice chart compilation from satellite images and principles of sea ice mapping and generation of digital ice chart data are described. Examples of ice charts compiled from

different satellite sensor systems are presented including the use of Geographical Information System (GIS) tools.

**Chapter 5** is devoted to studies of sea ice conditions in western and eastern parts of Eurasian Arctic seas. Regular use of satellite images for monitoring the Barents and Kara Seas began in the early 1970s, and after 1991 composite ice charts have been based on the optical and infrared range as well as side-looking radar (SLR) satellite imagery from the Russian *Okean* satellite. In spite of relatively coarse resolution they allow detection of ice edge, boundaries of landfast ice and polynyas and zones of different concentration and age with sufficient accuracy, including seasonal changes.

Satellite SAR data are used semi-operationally for studies of sea ice conditions in the NSR, and some results of these studies are described. The fast ice boundary in the western part of the Eurasian Russian Arctic and around Franz Josef Land was determined from *Radarsat* ScanSAR images for selected years. Furthermore, using *ERS* SAR and *Radarsat* ScanSAR images, the mean and standard deviations of polynya widths have been determined in the western Eurasian Arctic. Short-term, medium-term and long-term ice drift estimates were derived from successive satellite images for the Laptev Sea. The SAR imagery represents a unique capability for mapping ice drift in straits and near the coasts where other data sources provide limited information because of limited spatial resolution and cloudiness.

**Chapter 6** deals with semi-operational use of SAR data for supporting ice navigation. Since 1991 the Nansen Centers in Bergen and St. Petersburg together with Murmansk Shipping Company have demonstrated the use of SAR data for planning and selection of the navigation route in sea ice. Ten expeditions are described. In these expeditions *ERS-1/2*, *Radarsat* and *Envisat* SAR images were transmitted to icebreakers in near-real time to help them navigate in sea ice. This experience proves that high-resolution light- and weather-independent SAR images can be effectively used for both strategic and tactical support of icebreaker operations in sea ice. In 2004–2005 *Envisat* ASAR images for the western part of the NSR were routinely transmitted every 3 days to the MOH at the Murmansk Shipping Company, which selected and transmitted sailing routes to the nuclear icebreakers. Even in relatively easy sea ice conditions during winter–spring 2005 the average speed of ships in ice increased by about 30–40% as a result of using SAR data for ice routing.

The methodology of using SAR data onboard icebreakers for their tactical navigation in sea ice was also tested in many of the expeditions. It includes processing SAR raw data to make images, transmission of the images to icebreakers in the Northern Sea Route and their use by captains for ship routing. Experience of using satellite imagery in the optical and infrared band onboard the icebreakers is also described. Here, particular attention is drawn to the present technique of *NOAA* and *Meteor* imagery presentation onboard icebreakers in the Electronic Chart Display and Information System (ECDIS) of ship navigation.

The future of sea ice monitoring in the NSR should combine use of remote-sensing data in different spectral ranges, including routine use of SAR data, implementation of new information products for ice services and efficient distribution to users. Any future system of satellite monitoring for the purpose of ice navigation

should primarily be based on satellite data with a spatial resolution of at least 50–100 m and subject to daily coverage.

**Chapter 7** is devoted to the climatic variability of sea ice in the Arctic with the emphasis on the NSR. Long, continuous, observational data sets are necessary in order to investigate the long-term climatic fluctuations of sea ice. AARI data are the most comprehensive record for the Northern Sea Route and the greater Eurasian Arctic.

Overall, the interannual fluctuations of ice area in Eurasian Arctic seas during the 20th century indicate a gradual decrease through the century. However, interannual to multi-decadal variability in the ice cover area of the Arctic Ocean and its seas can also be characterized as having a quasi-periodic behavior on multiple time scales. AARI data analysis found these variations to be characterized by cyclic fluctuations with periods of 2–3, 5–7, 8–12 years and about 20 and 50–60 years, respectively.

Sea ice data sets derived from passive microwave data are among the longest continuous satellite-derived geophysical records, extending over the last quarter century. Analyses of merged SMMR–SSM/I data establish the decrease in Arctic sea ice area and extent (1978–2005) to be about ~3% per decade. Sea ice decrease in recent decades has been larger during summer, and September 2005 was the absolute minimum extent observed. A relatively large (~7% per decade) reduction in the multi-year ice area was found for the same period.

Knowledge of the long-term variability of ice cover in the Arctic Ocean and its marginal seas is of crucial scientific importance for climate study development, but also of strategic importance for planning shipping and other types of economic activities—such as gas and oil production in the Arctic, particularly in the Northern Sea Route.

The AARI authors of this book present sea ice scenarios for the 21st century using statistical models based on observed climatic variability of sea ice cover in the 20th century and predict that the ice extent will vary with a dominant period of 50–60 years reaching maximums around 2030–2040 and 2090–2095, respectively, and minimums in-between.

On the other hand, the Norwegian group of authors (Johannessen *et al.*, 2004) predict—by use of two coupled global climate models—that a reduction in the ice extent of 80% will occur during the summer as a result a doubling of CO<sub>2</sub> in the atmosphere and 20% during wintertime. These predictions are also strongly supported by the ACIA (2004). However, internal variability of the climate system—as observed with the strong warming event that peaked around 1940 and caused a major reduction in sea ice extent—can upset these predictions (Johannessen *et al.*, 2004). Finally, an assessment is made on how future climate will affect ice conditions in the Northern Sea Route.

The **Afterword** discusses present and future situations regarding gas and oil production and reviews other industrial activities, including the future use of the Northern Sea Route.